Publications of the Astronomical Society of the Pacific
91:589-607, October 1979

PUBLICATIONS OF THE
ASTRONOMICAL SOCIETY OF THE PACIFIC

Vol. 91 October 1979 No. 543

UBVRI PHOTOMETRY II: THE COUSINS *VRI* SYSTEM, ITS TEMPERATURE AND ABSOLUTE FLUX CALIBRATION, AND RELEVANCE FOR TWO-DIMENSIONAL PHOTOMETRY

M. S. BESSELL

Mount Stromlo and Siding Spring Observatories
Research School of Physical Sciences, Australian National University

The Cousins *VRI* system is proposed as an ideal system to adopt as the standard system for both Northern and Southern Hemisphere near-IR observations. Comparisons are made between $(b-y)$, $(G-R)_6$, $(V-I)_J$, and $(V-I)_c$ color indices measured for a large sample of equatorial HR stars which illustrate the precision of the system and the excellent temperature sensitivity of the $(V-I)_c$ index. Transformations between the different systems including the Eggen-Kron system are derived, a temperature calibration of $(b-y)$, $(R-I)_c$, and $(V-I)_c$ is provided based on empirical temperature determinations, and an absolute flux calibration for *UBVRI* is derived.

Photometry using photographic plates, electronic area detectors, and digital spectra is also discussed, and details given of specific photometric detector systems.

Key words: photometry—color indices—standard star systems—temperature calibrations

I. Introduction

The GaAs photocathode in the form of the RCA 31034A phototube has forced a reappraisal of the advantages of near-IR photometry in determining stellar temperatures for stars cooler than A0. The high quantum efficiency (QE) of the cathode compared to that of the Sl photocathode enables faint stars to be measured with ease using small to medium telescope apertures, and this high sensitivity together with the small extinction corrections and apparent tube and filter stability has permitted the establishment of broad-band standards with precision once believed possible only with narrow-band filters. Three near-IR systems have undergone development or modification over the past few years using this tube. These are the Washington system (T_1-T_2): (Canterna 1976); the Eggen-Kron system $R_K,(R-I)_K$: Eggen (1975, 1978); and the Cousins system V, $(V-R)_c$, $(R-I)_c$, $(V-I)_c$: Cousins (1976*a*,*b*, 1978*a*). Bessell (1976) (Paper I) and Bessell and Williams (1976) have discussed these systems and the use of a GaAs tube and glass filters to duplicate existing broad-band systems.

Apart from the work of Canterna and collaborators in the (T_1-T_2) system, and Weistrop (1975) in the $(R,I)_K$ system most of the recent near-IR photometry has taken place in the Southern Hemisphere using standard stars not accessible from the north. However, it has been reported that Kunkel and Rydgren (1979), Landolt (1978), and Crawford (1978) are independently establishing equatorial V, R, I standards from the Landolt (1973) catalog (using GaAs tubes and glass filters) which will be suitable for Northern Hemisphere photometry. The majority of these observations have not been transformed into any existing standard system but have been maintained on the different natural systems which will permit the internally precise values to be eventually transformed accurately into a well-defined standard system.

It is particularly important to resist the proliferation of different standard systems and to attempt to obtain agreement on a single system, its filters, and standards. The existence of different but similar systems leads to unnecessary confusion in the literature and much wasted photometric effort. In many cases the transformation of color indices from one system to another is made inaccurate by uncertainties in the defining subsets of "standards."

The Cousins system appears for several reasons to be the most suitable of existing systems to adopt as the standard. It is the only near-IR system which is well defined for blue as well as red stars; it uses the Johnson V magnitude as its base magnitude; the color indices of the primary standards are defined to several thousandths of a magnitude; it is the natural system of the RCA 31034A tube and glass filters which are readily available and similar to those commonly in use. Another important consideration is that Graham (1979) is extending the Cousins system to the faint E-region

stars and field M dwarfs so that they will be directly accessible to large Southern Hemisphere telescopes.

To facilitate the extension of this system to the Northern Hemisphere, Cousins (1979) has kindly made available a list of 280 equatorial standards of all spectral types. These stars were not intended as standards for the system (not being as precise as the E- and F-region stars) but they are determined to better than $0^m.01$ and there are many of them so they should ensure an accurate transference of the system to the north.

Many of the brightest HR stars in this list have also been observed in other photometric systems. In the following sections we will examine the transformation between the Cousins $(V-I)_c$ and $(R-I)_c$ color indices and the $(b-y)$, $(G-R)_6$ $(V-I)_J$, $(R-I)_K$, and (T_1-T_2) indices of the Strömgren four-color, the Kron six-color, the Johnson ten-color, the Eggen-Kron (R,I), and the Washington systems. The precision of the defining color-system catalogs will also be assessed. An effective temperature calibration for the $(b-y)$, $(V-I)_c$, $(R-I)_c$ indices will be derived based on the Code et al. (1976) fundamental temperatures for the hotter stars ($T >$ 5800 K) and on the Ridgway et al. (1979) temperature scale for the cooler stars.

Finally the advantages of $(V-I)$ photometry using glass filters and area detectors such as sensitized photographic plates, imaging photocathode devices, and CCD arrays are discussed.

II. Comparison of Different Color Systems

A. *The Cousins System*

In Figures 1a and 1b are shown the correlation between $(R-I)_c$ and $(V-I)_c$ for B–G stars and K–M stars, respectively. The relationship is nonlinear but shows a tight correlation with practically all the points lying within $\pm 0^m.005$ of the mean line for those stars earlier than K, and with the scatter approximately doubling for those stars redder than K. The change in $(V-I)_c$ is more than twice that of $(R-I)_c$ for the A–F stars and about 1.5 times the $(R-I)_c$ variation for the late K–M stars.

The tightness of the correlation between $(R-I)$ and $(V-I)$, and the relations between instrumental color indices and standard indices should not be sensitive to the exact location of the V, R, and I bands except in the M stars where the TiO bands become strong. That is, nonstandard filters should produce precise linear transformations for the weak-band stars but will show nonlinearities and higher external scatter for the later-type stars.

B. *The Four-Color Index* $(b-y)$

In Figure 2 are plotted the $(b-y)$ and $(V-I)_c$ color indices for 84 bright stars. The $(b-y)$ indices are from Crawford and collaborators as listed in the Lindemann and Hauck (1973) catalog; supergiant OB stars and K giants are not plotted. The transformation is again not linear but shows excellent correlation with almost all the points lying within ± 0.010 magnitude of the mean line. The transformation can be approximated by three linear relations

$$(V-I)_c = 2.60\,(b-y) + 0.02, \qquad (b-y) < -0.05$$

$$(V-I)_c = 2.12\,(b-y) \qquad , -0.05 < (b-y) < 0.12$$

$$(V-I)_c = 1.53\,(b-y) + 0.075, \qquad 0.12 < (b-y) < 0.60$$

which are valid for dwarfs of spectral types B, A–F, F–K, respectively. The O, B, A, and F supergiants are known to show different $(b-y)$ color indices to dwarfs because of the effect of gravity on the blue colors. Eggen (1978) has found a similar effect in the K stars and derives different $(b-y)$, $(R-I)_K$ relations for G–K giants and dwarfs in old clusters and groups. Because the $(V-I)_c$ index is less affected by both metal line blanketing and by gravity-induced color changes than are $(B-V)$ or $(b-y)$ (Bessell and Wickramasinghe 1979), and because it is more than twice as sensitive to temperature changes than is $(b-y)$, $(V-I)_c$ is an ideal index to use in determining the temperature of A–G stars (see also Crawford 1979).

C. *The Six-Color Index* $(G-R)_6$

There were 53 stars in the catalog of Kron, Guetter, and Riepe (1972) common to the Cousins list. The 40 stars bluer than $(V-I)_c = 0.90$ are plotted in Figure 3. Bluer than $(V-I)_c = 0.70$, 66% of the points lie within ± 0.015 magnitude of the mean line, and all points lie within ± 0.025 magnitude of the line. For those stars redder than $(V-I)_c = 0.7$, the scatter is approximately doubled. A single linear transformation fits the whole color range

$$(V-I)_c = 1.5(G-R)_6 + 0.75 \quad .$$

D. *The Johnson* $(V-I)_J$, $(R-I)_J$, *and* $(V-R)_J$ *Indices*

Figures 4a and 4b show the $(V-I)_J$ and $(R-I)_J$ versus $(V-I)_c$ and $(R-I)_c$ diagrams, respectively, for stars in the Johnson et al. (1966) catalog. The $(V-I)$ transformation can be approximated by three linear relations

$$(V-I)_c = 0.713\,(V-I)_J \quad , \qquad (V-I) < 0$$

$$(V-I)_c = 0.778\,(V-I)_J \quad , \qquad 0 < (V-I)_J < 2.0$$

$$(V-I)_c = 0.835\,(V-I)_J - 0.13, \quad 2.0 < (V-I)_J < 3.0 \quad .$$

The $(R-I)$ transformation cannot be approximated with a few linear relations, but is best described by a single linear relation with a nonlinear correction curve (Fig. 4c). The transformation is

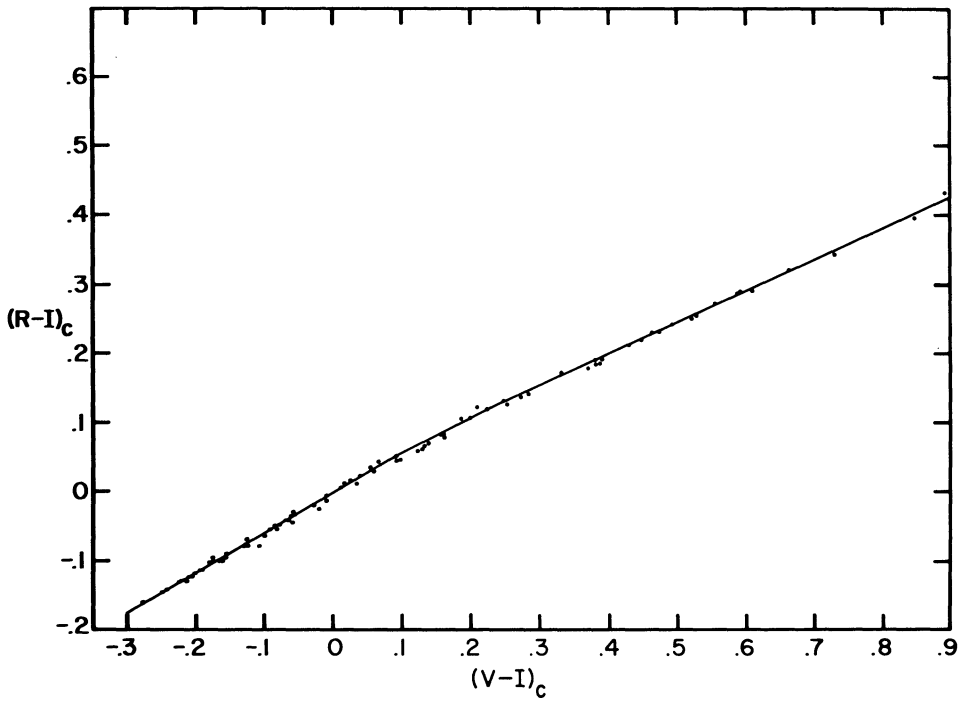

FIG. 1a—$(R-I)_c$ versus $(V-I)_c$ from the list of Cousins (1979) equatorial stars between ± 10° declination.

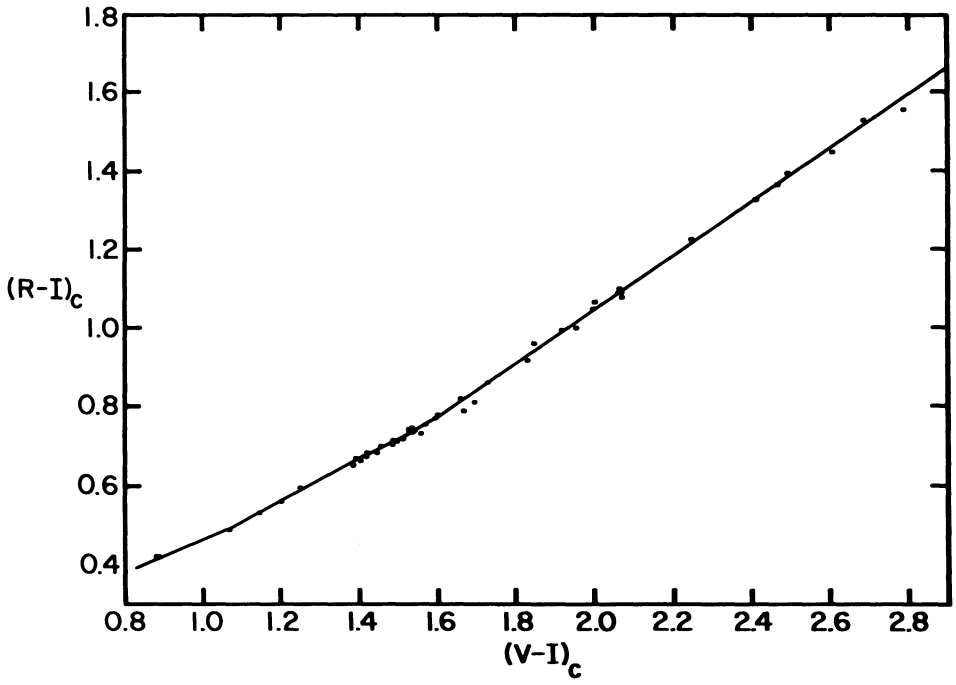

FIG. 1b—$(R-I)_c$ versus $(V-I)_e$ from the list of Cousins (1979) equatorial stars between ± 10° declination.

$$(R-I)_c = 0.856\,(R-I)_J + 0.025 + \Delta(R-I)_J \quad .$$

The $(V-R)$ transformation (not plotted) can be approximated by two linear relations

$$(V-R)_c = 0.73\,(V-R)_J - 0.03, \qquad (V-R)_J < 1.0$$

$$(V-R)_c = 0.62\,(V-R)_J - 0.08, \quad 1.0 < (V-R)_J < 1.7 \ .$$

The $(R-I)_J$ data appear the most precise with the majority of points lying within ±0.017 magnitude of the mean line; Crawford (1979) deduced a similar scatter from a comparison of $(b-y)$ and $(R-I)_J$. The $(V-I)_J$

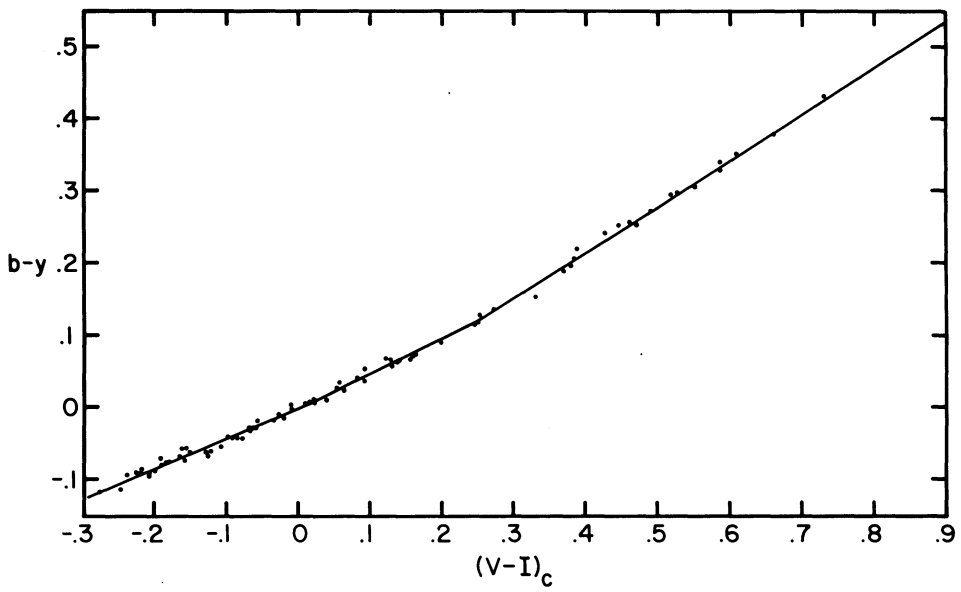

FIG. 2—$(b-y)$ (Crawford and associates: Lindemann and Hauck, 1973) versus $(V-I)_c$.

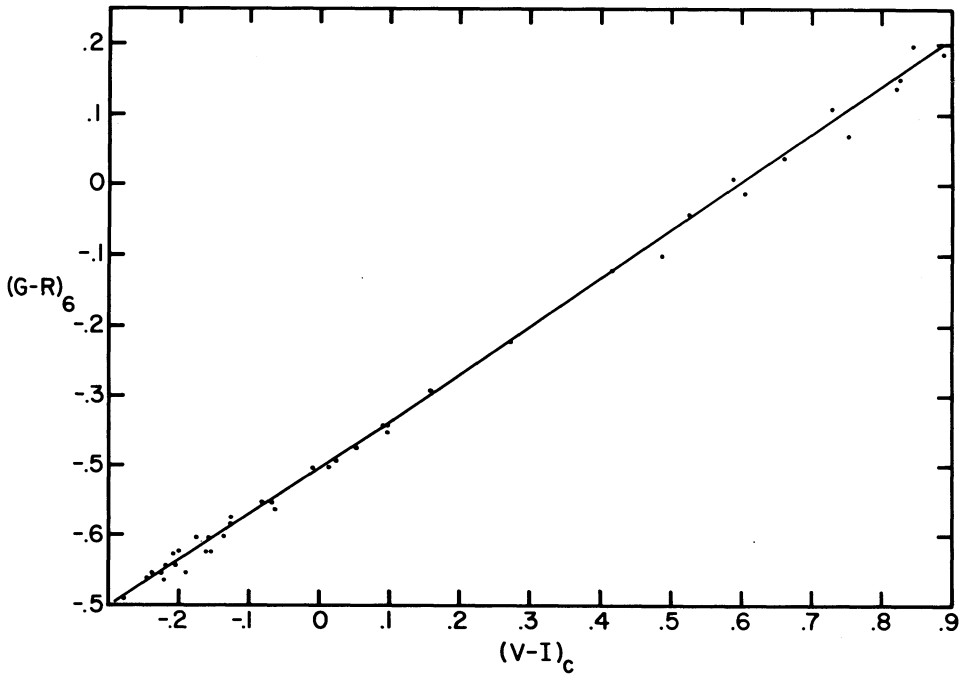

FIG. 3—$(G-R)_6$ (Kron, Guetter, and Riepe 1972) versus $(V-I)_c$.

and $(V-R)_J$ values show a scatter of $\pm 0^m.03$ and $\pm 0^m.025$, respectively.

Johnson (1965) has also presented color indices for 43 K and M dwarfs. From 32 stars in common with Eggen (1979) and six with Cousins (1979),

$$(R-I)_K = 0.807\,(R-I)_J - 0.055, \quad 0.30 < (R-I)_K < 1.4$$

$$(R-I)_c = 1.005\,(R-I)_J - 0.036, \quad 0.60 < (R-I)_c < 1.6$$

The two stars redder than $(R-I)_K = 1.4$, Y 2553 (W359) and Y 2582B, deviate from the linear relation.

This relation between $(R-I)_c$ and $(R-I)_J$ defined by the K and M dwarfs differs from that defined by the bright equatorial stars shown in Figure 4b. The $(R-I)_J$ values of the dwarfs (plotted as crosses) are systematically bluer by about 0.05 magnitude. Kunkel (1979, private communication) has also commented from his photometry that the Johnson (1965) *VRI* system did not match the Johnson et al. (1966) bright-star *VRI* system.

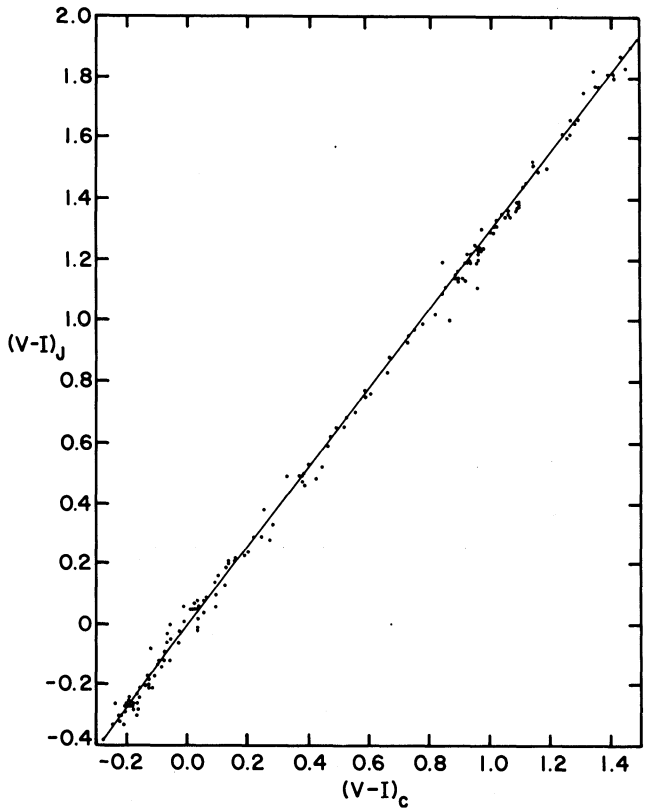

FIG. 4a—$(V-I)_J$ versus $(V-I)_c$ (Johnson et al. 1966). Crosses are data from Johnson (1966).

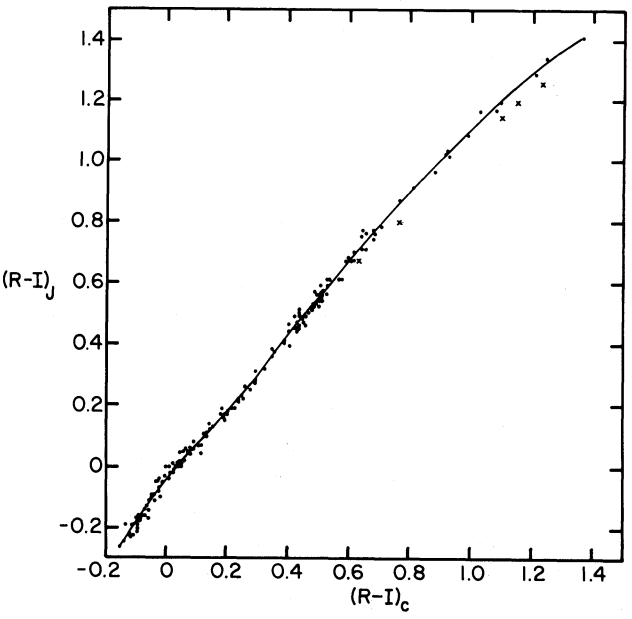

FIG. 4b—$(R-I)_J$ versus $(R-I)_c$ (Johnson et al. 1966). Crosses are data from Johnson (1966).

E. *The Kron-Eggen System*

There are 36 stars in the Kron, Gascoigne, and White (1957) R_K, $(R-I)_K$ catalog of nearby stars and there are 16 of Eggen's R_K, $(R-I)_K$ standards which

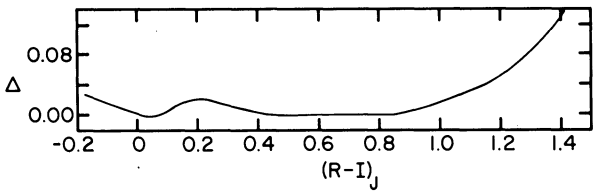

FIG. 4c—Δ versus $(R-I)_J$. See text for explanation of Δ.

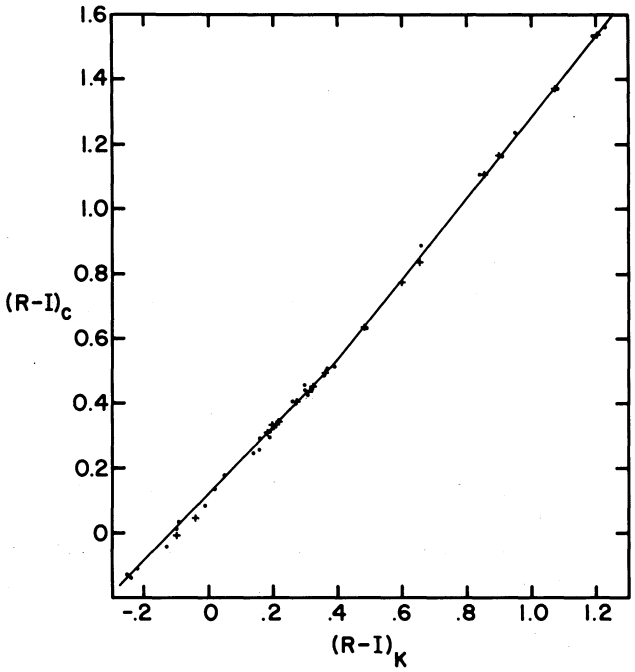

FIG. 5—$(R-I)_c$ versus $(R-I)_K$. Solid circles Kron, Cascoigne, and White (1975); crosses Eggen (1978).

are in common to Cousins' equatorial list. In Figure 5 the $(R-I)_c$ versus $(R-I)_K$ values are plotted. Eggen's version of $(R-I)_K$ is seen to duplicate the Kron et al. (1957) system very precisely except for the two bluest stars which appear to be systematically redder by about 0.02 magnitude. The precision of the Kron et al. (1957) $(R-I)_K$ indices is between $0^m.01$ and $0^m.02$, which is the accuracy claimed for the majority of stars; the Eggen $(R-I)_K$ standards are better than 0.01 magnitude. Two linear relations transform $(R-I)_K$ to $(R-I)_c$

$$(R-I)_c = 0.118 + 1.03\ (R-I)_K,\quad (R-I)_K < 0.35$$

$$(R-I)_c = 0.033 + 1.246\,(R-I)_K,\ 0.35 < (R-I)_K < 1.30.$$

Although neither Kron et al. nor Eggen derived $(V-I)_K$ as an observed color index, it can be constructed from $(V-I)_K = V-R_K + (R-I)_K$.

Figure 6 shows $(V-I)_K$ versus $(V-I)_c$. Within the expected errors, two linear approximations are valid

$$(V-I)_c = 0.27 + 0.936\,(V-I)_K,\quad (V-I)_K > 0.5$$

$$(V-I)_c = 0.24 + 1.00\ (V-I)_K,\quad (V-I)_K < 0.5\ .$$

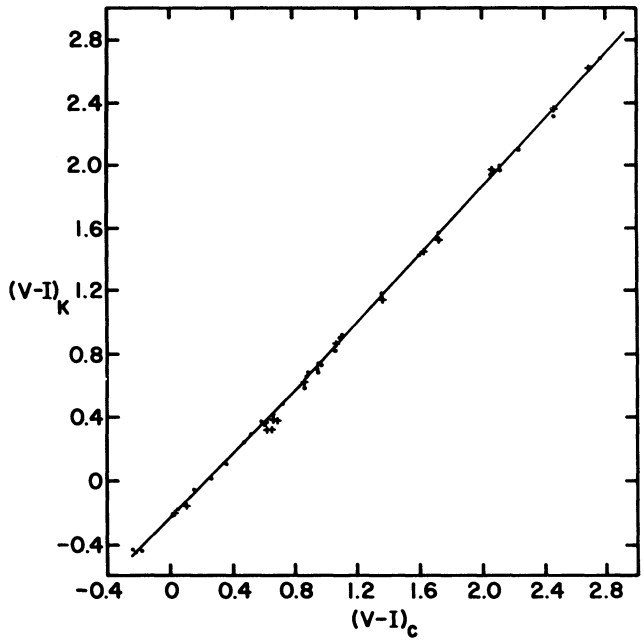

FIG. 6—$(V-I)_K$ versus $(V-I)_c$. Symbols as above, but see text for explanation of $(V-I)_K$.

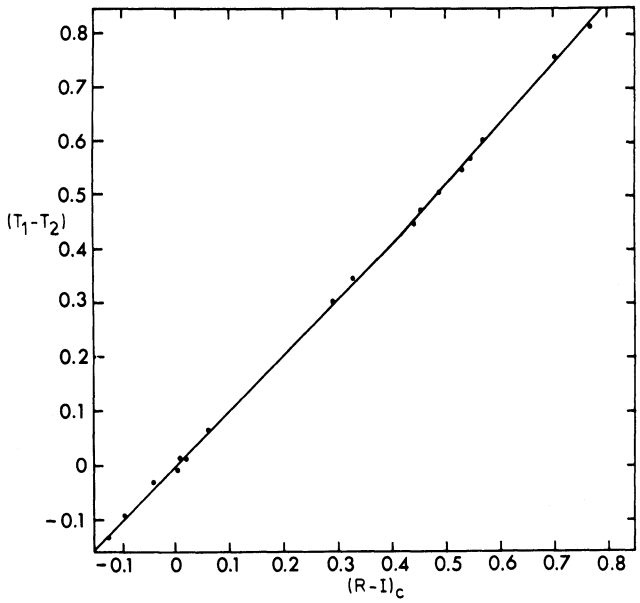

FIG. 7—(T_1-T_2) (Canterna 1976) versus $(R-I)_c$.

The $(V-I)_K$ values derived from the Eggen standards appear to diverge systematically from the Kron et al. points; however, this is mainly a selection effect because comparison of the $(V-I)_K$ values for the larger group of 32 stars common to Kron and Eggen weakens the trend and increases the scatter.

F. *The Washington* (T_1-T_2) *System*

There are only 15 stars common to Canterna (1976) and Cousins; these are shown in Figure 7. Because the zero points of both systems were chosen so that the indices were zero for stars with $(B-V) = 0$, the relation between $(R-I)$ and (T_1-T_2) should pass through (0,0). Two linear relations describe the transformation:

$$(R-I)_c = 0.980\,(T_1-T_2) \quad , \quad -0.15 < (T_1-T_2) < 0.40$$

and

$$(R-I)_c = 0.875\,(T_1-T_2) + 0.044,$$

$$0.40 < (T_1-T_2) < 0.85 \quad .$$

The mean error given by Canterna (1976) for the 15 stars used was 0.013 magnitude but the majority of the stars plotted lie within 0.005 magnitude of the lines. The (T_1-T_2) system is evidently a very precisely defined system.

Canterna and Harris (private communication) have now measured some stars in V and $(V-T_1)$. Five stars in common with Cousins give the following transformations,

$$(V-R)_c = 0.98\ (V-T_1) + 0.015, \qquad 0 < V-T_1 < 0.30$$

$$(V-R)_c = 1.082(V-T_1) - 0.014, 0.30 < V-T_1 < 0.85\ .$$

G. *The U.S. Naval Observatory* $(V-I)_{KM}$ *System*

Conard Dahn and Harry Guetter (1979 private communication) have refined the standards of the Kron-Mayall (1960) system using an S1 tube and the original filters to produce standard values accurate to a few thousandths of a magnitude. The 38 stars in common with Cousins are plotted in Figure 8a. They yield a transformation of

$$(V-I)_c^\circ = 0.188 + 0.946\,(V-I)_{KM},$$

$$-0.4 < (V-I)_{KM} < 2.5 \quad .$$

However, the points deviate systematically from this line as seen in Figure 8b, and the more precise relation is

$$(V-I)_c = (V-I)_c^\circ + \Delta(V-I)_{KM} \quad .$$

The nonlinearity for $-0.5 < (V-I)_{KM} < 0.5$, which is also apparent in the $(R-I)_J$ transformation, is due to the I passband of the S1 systems straddling the Paschen discontinuity, whereas the I band of the GaAs systems is mainly shortward of this feature. The nonlinearity for the later-type M stars is caused by the abrupt redward shift in effective wavelength of the S1 I bands as the TiO absorption increases. Bessell (unpublished) has measured color indices in the Cousins system for G176–12, W359, and G51–15, the reddest stars in the Dahn and Guetter list. Inclusion of these stars in the comparison yields for $2.2 < (V-I)_{KM} < 4.3$

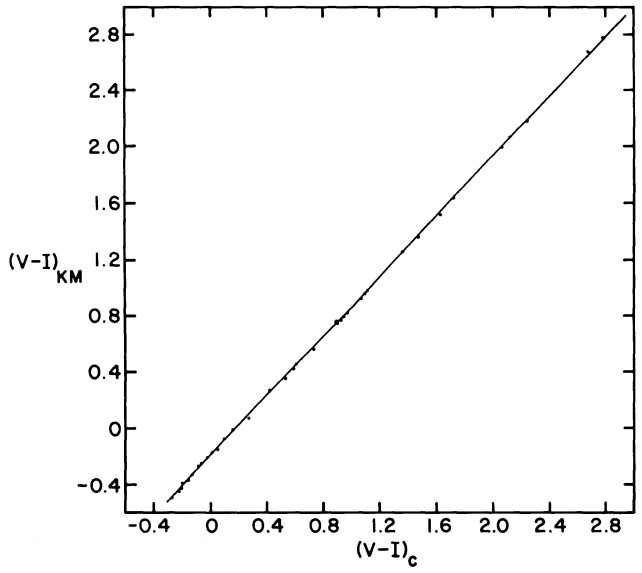

FIG. 8a—$(V-I)_{KM}$ (Dahn and Guetter, 1979) versus $(V-I)_c$.

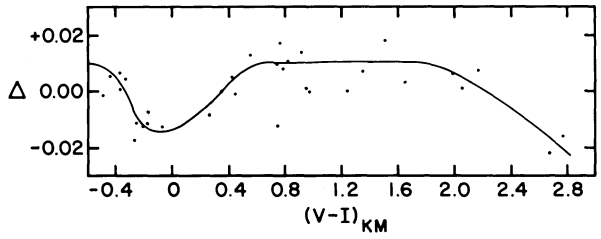

FIG. 8b—Δ versus $(V-I)_{KM}$. See text for explanation of Δ.

$$(V-I)_c = 0.91\,(V-I)_{KM} + 0.26 \quad .$$

H. $(r-rg9)$ *and* $(R-I)_{PUJ}$

Argue (1967) and Jacobsen (1970) have also observed R and I colors with Sl tubes. The color indices of those stars in common with Cousins are shown in Figure 9. The transformations are nonlinear for the reasons given above, but the precision of the bulk of the Argue and Jacobsen data is better than ± 0.01 magnitude.

1. Kunkel and Rydgren (1979) have published color indices for M dwarfs and faint equatorial stars observed with a GaAs photomultiplier. Their photometry appears excellent. A comparison of stars common to Kunkel and Rydgren (1979), Cousins (1979), Eggen (1979), and Bessell (1979 unpublished) yields

$$(R-I)_K = 1.01\,(r-i) - 0.155 \quad \text{(26 M stars only)},$$

and from 20 stars of all spectral types

$$(R-I)_c = 1.12\,(r-i) \quad , \qquad (r-i) < 1.0$$

$$(R-I)_c = 1.233\,(r-i) - 0.133, \qquad (r=i) > 1.0$$

and

$$(V-I)_c = 1.02\,(V-i) + 0.03 \quad , \qquad (V-i) < 1.6$$

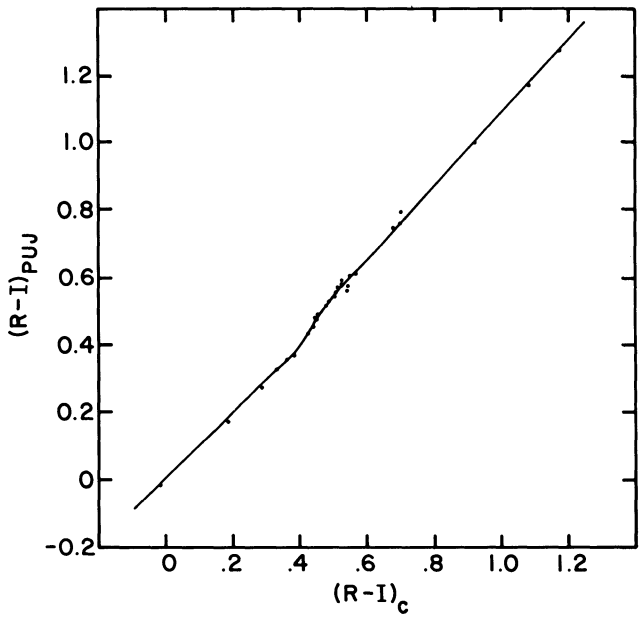

FIG. 9a—$(R-I)_{PUJ}$ (Jacobsen 1970) versus $(R-I)_c$.

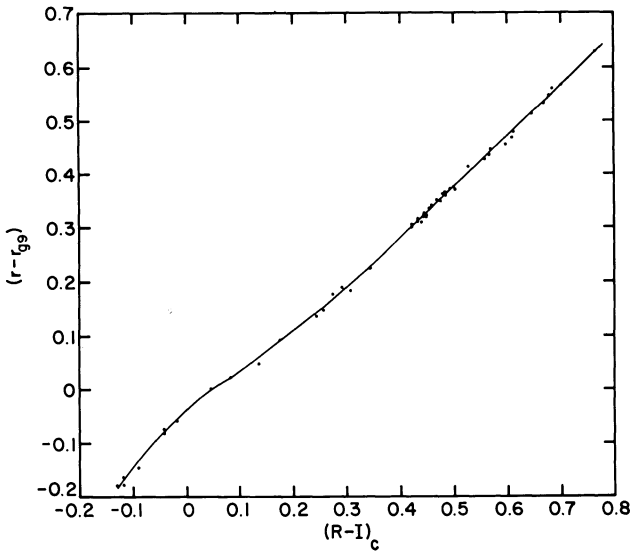

FIG. 9b—$(r-rg9)$ (Argue 1967) versus $(R-I)_c$.

$$(V-I)_c = 0.96\,(V-i) + 0.13 \quad , \qquad (V-i) > 1.6 \quad .$$

III. The Temperature Calibration

Code et al. (1976) have defined an essentially empirical effective temperature scale for early-type stars based on angular diameters, measured with the Narrabri stellar interferometer and absolute flux distributions. This scale was used by Davis and Shobbrook (1977) to determine the temperature calibration of the four-color $[u-b]$ and c_0 indices for O and B stars. The cooler stars in the Code et al. list can be used similarly to derive a temperature scale for the A–G stars using

more appropriate color indices.

In Table I are presented the relevant data for the calibrating stars. There being few $(V-I)_c$ values for these stars, the $(b-y)$ values are the most accurate color indices suitable for the temperature determination in A–G stars. The $(b-y)$ and $[u-b]$ $(= c_1 + 2m_1 + 0.4(b-y))$ color indices are taken from the list of Crawford and collaborators, cited above. The relation for B stars, $(b-y)_0 = 0.087\ [u-b] - 0.125$, which can be derived from Shobbrook (1976), was used to compute the alternate values of $(b-y)$ given in the sixth column using the more temperature-sensitive $(u-b)$ color index. The agreement between the measured and computed $(b-y)$ values for the hotter stars is encouraging. The average $(b-y)$ value for these stars is plotted in Figure 10. Both $(G-R)_6$ and $(V-I)_J$ color indices have been measured for the sun. The $(b-y) = 0.395$ value given in Table I was the average of the two $(b-y)$ color indices obtained after transforming the measured indices using the dwarf relationships. The $(b-y)$ calibration for dwarfs hotter than 5500 K given in Table II was read from the smooth eye-fitted line in Figure 10. The $(b-y)$ values for the cool dwarfs was derived from the $(b-y),(R-I)_K$ relationship given by Eggen (1977) for Wolf 630 group dwarfs and from unpublished observations by Bessell for M dwarfs.

For giant stars cooler than the sun a temperature scale is available from the work of Ridgway et al. (1979). Their temperature scale derived for luminosity class III stars is based on radii measured by lunar occultation. They give the relation between effective temperature, near IR continuum temperature and $(V-K)$ color index. The relation between $(V-I)$ and $(V-K)$ provided the temperature calibration given in Table III. Apart from YY Geminorum, an eclipsing binary, no radii are known for M dwarfs. Veeder (1974) determined temperatures for M dwarfs by fitting blackbody curves to their broad-band energy distributions between 0.4 μ and 3.5 μ.

For temperatures hotter than 3100 K his derived $(V-K)$ and $(R-I)$ versus *blackbody*-temperature relations are in good agreement with the $(V-K),(R-I)$ versus (0.7 μ–1.0 μ) *continuum*-temperature relations derived by Ridgway et al. (1979) for giants. Because the atmosphere structure and opacities in the giants and dwarfs are quite different due to the different gravities of the stars, there is no a priori reason to believe that the same effective temperature, color relation should hold for giants and dwarfs. In fact, the theoretical effective temperature, color relations of Mould and Hyland (1976) predict that the effective temperatures of M dwarfs are cooler than the continuum temperatures, which is opposite to the effect measured for giants by Ridgway et al. (1979) or predicted by the giant models of Tsuji, Bell, and Gustaffson (Ridgway et al. 1979).

However, the coolest ($3500\ \mathrm{K} > T > 3000\ \mathrm{K}$) models of Mould (1976), which predict the only significant temperature differences (> 100 K), are uncertain because the H_2O opacity has been overestimated (Persson, Aaronson, and Frogel (1977) and as H_2O is an important opacity source in these M dwarfs (Auman, 1969) any conclusions regarding effective temperatures and colors will be affected. Because of these uncertainties, we have given in Table II Veeder's blackbody-temperature scale for the M dwarfs. The true effective temperature scale for these stars must await further work. For dwarfs with temperatures between 4000 K and that of the sun the effective temperature,$(V-I)$ relation of the giants was assumed. This is a good ap-

TABLE I

DATA FOR CALIBRATION STARS

HR	Name	Sp	b-y	[u-b]	$(b-y)_o$	Log T_e	se
	Sun	G2 V	0.395			3.762	
2421	γ Gem	A1 IV	0.007	1.486	0.004	3.967	±0.014
2491	α CMa	A1 V	-0.004	1.253	-0.016	3.999	0.007
2943	α CMi	F5 IV	0.272			3.814	0.008
3685	β Car	A1 IV	0.004	1.553	0.010	3.966	0.010
3982	α Leo	B7 Vn	-0.041	0.900	-0.047	4.087	0.011
4534	β Leo	A3 V	0.044			3.947	0.016
4662	γ CrV	B9P	-0.043	0.955	-0.042	4.095	0.018
5056	α Vir	B1 IV	-0.114	0.07	-0.119	4.379	0.15
6556	α Oph	A5 III	0.093			3.904	0.018
6879	ε Sgr	A0 V	0.016	1.386	-0.004	3.976	0.010
7001	α Lyr	A0 V	0.004	1.405	-0.003	3.985	0.006
7557	α Agl	A7 IVn	0.137			3.904	0.011
7790	α Pav	B2.5 V	-0.092	0.408	-0.090	4.252	0.017
8425	α Gru	B7 IV	-0.061	0.762	-0.059	4.148	0.016
8728	α PscA	A3 V	0.036			3.944	0.015

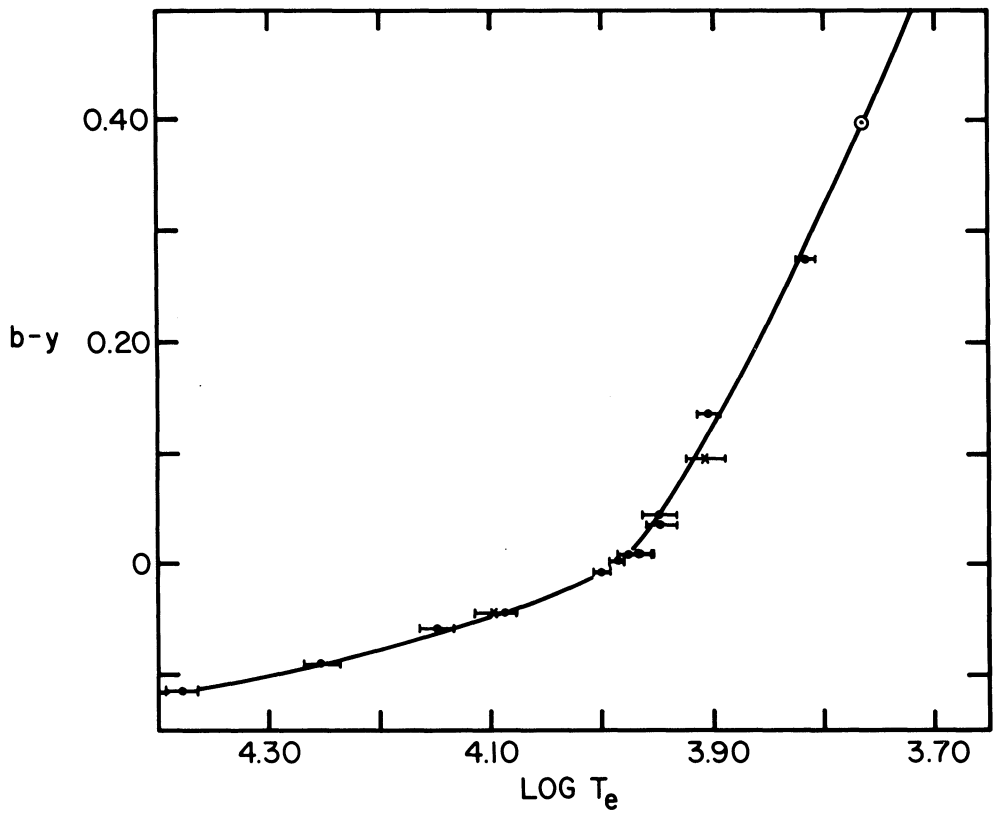

FIG. 10—Effective temperature, $(b-y)$ relation for early-type stars.

TABLE II

TEMPERATURE CALIBRATION FOR NORMAL DWARFS

T_e	b-y	B-V	$(V-I)_c$	$(R-I)_c$	MK
13000	-0.054	-0.14	-0.120	-0.070	B7 V
12000	-0.041	-0.10	-0.085	-0.050	B8 V
11000	-0.027	-0.065	-0.055	-0.032	B9 V
10000	-0.010	-0.025	-0.020	-0.012	A0 V
9500	0.007	0.005	0.015	0.008	A1 V
9000	0.035	0.055	0.072	0.040	A2 V
8500	0.072	0.14	0.155	0.084	A5 V
8000	0.118	0.22	0.250	0.132	A7 V
7500	0.165	0.275	0.330	0.168	F0 V
7000	0.220	0.35	0.415	0.207	F2 V
6500	0.286	0.45	0.515	0.250	F5 V
6000	0.360	0.57	0.625	0.303	G0 V
5500	0.445	0.70	0.760	0.364	G6 V
5000	0.535	0.88	0.93	0.43	K2 V
4500	0.60	1.02	1.11	0.51	K4 V
4000	0.80	1.32	1.53	0.74	K7 V
4000*	0.82	1.34	1.57	0.76	K7 V
3500*	1.01	1.53	2.19	1.18	M2 V
3000*	1.22	1.74	3.03	1.77	M4.5 V
2750*	1.37	2.0+	3.58	2.18	M6 V

*Black body temperatures. Veeder (1974).

proximation, as one would expect the $(V-I)$ or $(R-I)$ color indices to show little change with the small gravity difference between GK stars of luminosity class III and V.

IV. Absolute Calibration of Photometry

Table IV lists an absolute calibration of *UBVRI* and 104 photometry which was derived using the relative absolute energy distribution of eight Hayes (1970) standards and the absolute flux calibration for α Lyrae given by Hayes and Latham (1975). Details are given in Appendix 2. The $(U-V),(B-V)$ calibration is in good agreement with that given by Johnson (1966).

V. Reddening and Intrinsic Lines in the Cousins *BVRI* System

Cousins (1978*b*,*c*) has discussed the intrinsic color indices of dwarfs (class V), giants (class III), and supergiants in the Cousins *BVRI* system. The derived values can be found in tables or figures given in these papers.

Reddening relations were also derived (Dean, Warren, and Cousins 1978; Appendix); these are

$$\frac{E(V-I)}{E(B-V)} = X[1 + 0.06(B-V)_0 + 0.014\,E(B-V)]$$

$$E(B-V) = E_0[1 - 0.08(B-V)_0]$$

when

$$X = \frac{E(V-I)}{E(B-V)} \quad \text{for a star with } E(B-V) \to 0$$

and $(B-V) = 0$, and E_0 is the colored excess for a star

TABLE III

TEMPERATURE CALIBRATION FOR NORMAL GIANTS

T_e*	T_c*	b-y	B-V	$(V-I)_C$	$(R-I)_C$	(V-K)*	MK*
5000	4980	0.55	0.89	0.93	0.433		G7 III
4750	4730	0.60	0.98	1.00	0.461	2.31	K0 III
4500	4460	0.68	1.11	1.11	0.510	2.60	K2 III
4250	4140	0.80	1.26	1.28	0.600	2.96	K3 III
4000	3890	0.90	1.43	1.53	0.735	3.47	K5 III
3750	3560	1.00	1.62	1.97	1.025	4.24	M2 III
3500	3160			2.76	1.570	5.42	M4.5 III
3250	2580			3.80		6.84	M6 III

*From Ridgway, Joyce, White, Wing (1979)

TABLE IV

ABSOLUTE CALIBRATION OF PHOTOMETRY

Filter band	λ_0	Absolute flux density for mag = 0.00 F_ν
U	0.36 μ	1.81×10^{-23} W m^{-2} hz^{-1}
B	0.44 μ	4.26×10^{-23}
V	0.55 μ	3.64×10^{-23}
R_C	0.64 μ	3.08×10^{-23}
I_C	0.79 μ	2.55×10^{-23}
104	1.04 μ	2.00×10^{-23}
K	2.2 μ	6.49×10^{-24}

of $(B-V) = 0$.

VI. Instrumentation Considerations

A. *Filters*

The broad-band *UBVRI* passbands are defined by colored-glass combination filters and the sensitivity cut-off of the photocathodes. The filters not used are similar to those discussed by Bessell (1976), the changes permitting closer alignment to Cousins' natural system (see Appendix 1 for details).

These filters are

U	1 mm UG 2	+ $CuSO_4$
B	1 mm BG 12	+ 2 mm GG 385 + 1 mm BG 18
V	2 mm GG 495	+ 1 mm BG 18
R	2 mm OG 570	+ 2 mm KG3
I	3 mm RGN 9	.

The red-leak-blocking $CuSO_4$ filter can either be a liquid cell described in Paper 1, or a solid crystal filter obtainable from Interactive Radiation, New Jersey.

Most astronomical detectors used for precision observations are optimized for the faintest objects and are run at a fixed maximum gain setting. This mode of operation invariably results in many objects being too bright to measure directly, because of the possibility of detector damage or because of nonlinearities at high counting rates. A practical solution to this general problem is the use of neutral density filters. Many such absorbing filters commonly available are not very neutral, but show quite different attenuation with wavelength and have therefore not been used much in quantitative work. However, some metallic-alloy-coated, fused-silica filters manufactured by Oriel can be selected with constant attenuation to within 3% from 0.3 μ to 1 μ. Such filters would cause no effective wavelength shifts and only small reproducible zero-point shifts in the derived broad-band colors. Care should be taken, however, to avoid problems associated with light reflected from the filter.

B. *Photometric Methods*

It is possible that traditional Fabry-imaging photometry of individual objects will be increasingly replaced by multi-image filter photometry or by computer synthesis of color indices from digital spectra. In the first technique, many stars will be observed simultaneously in one color with an area detector at the focus of a direct camera; in the second, many colors will be "observed" simultaneously for one object with an area detector at the focus of a spectrograph camera.

The advantages of traditional photometry are simplicity, linearity, large dynamic range, high sensitivity, stability, and precision. The disadvantages are a requirement of photometric skies, a restriction to single-star observation, and an inability to work accurately with the small apertures necessary in crowded or high-sky-background fields. Area detectors admirably overcome these disadvantages but have great difficulty

matching the advantages, most importantly the precision and dynamic range. Synthesized indices from digital spectra can be measured with precision over a restricted dynamic range but wide wavelength coverage is usually limited by the grating blaze efficiency and off-axis vignetting of the spectrograph. The unique advantage of digital spectra however lies in the versatility of being able to compute color indices in any photometric system, as well as having spectral line and band information.

VII. Detector Systems

In Figure 11 are shown the relative spectral sensitivity curves (on a linear scale) for examples of three types of detectors currently in use: photomultipliers, imaging electronic detectors, and hypersensitized Kodak photographic plates (Kodak 1973). Also shown (plotted in units of Rayleighs per Å) is the smoothed (~ 100 Å) night-sky spectrum (Broadfoot and Kendall 1968), the brightness of which effectively limits the signal-to-noise ratio of ground based photometry of faint astronomical objects.

A. *Photomultipliers*

Table V lists data for three advanced tubes widely used in astronomy. Extended-red S20 photocathodes such as in the selected EMI 9658 *R* or 9659 *B* tubes can be used very successfully for *UBVRI* photometry. The effective wavelengths of the *V*, *R*, and *I* passbands obtained with the extended S20 differs only slightly from those obtained with the GaAs tube (Cousins 1974) and the standard star color indices transform precisely. There may however be small differences between the $(R-I)$ indices of extremely weak-line and strong-line K stars measured with some *R* filters and different cathodes. The 9658 *R* tube has a novel feature, its end window having an internal surface of pyramid-shaped prisms onto which the photocathode is deposited. This apparently increases the quantum efficiency in the 0.3 μ–0.9 μ region without significantly affecting the dark current.

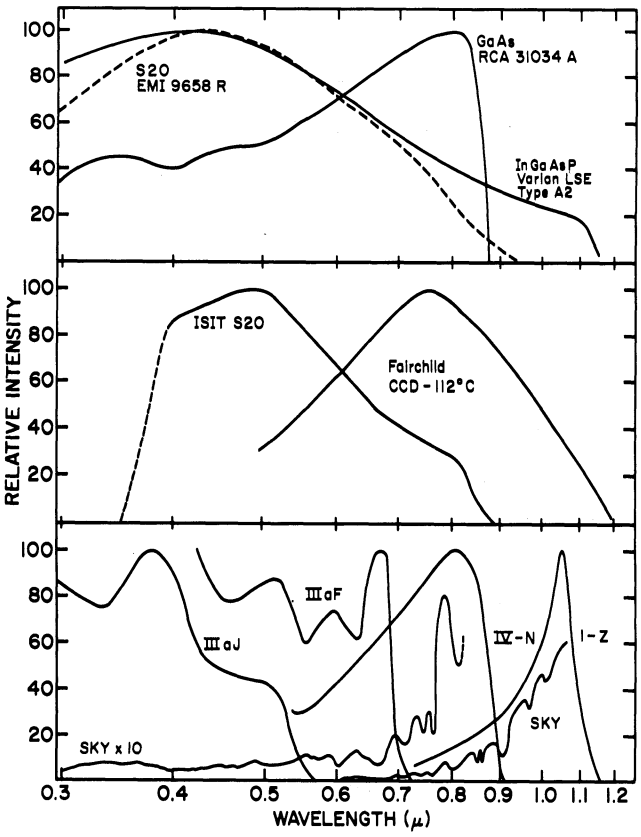

FIG. 11—Relative sensitivity curves for various detectors described in text.

The very red-sensitive RCA 31034 A tube is the "natural" tube of the Cousins *VRI* system and the Eggen-Kron *R,I* system. Cousins uses the tube at $-10°$ C while most other observers use dry-ice cooling at ~ $-78°$ C which produces slightly lower dark counts and a bluer red cutoff. Peculiarities of the tube are the low maximum permitted anode current of 0.1 μÅ (compared to 1 μÅ for the Varian tube and ~ 200 μÅ for the EMI tube) which corresponds to a count rate for some tubes of about 300,000 at a gain of 10^6; a hysteresis in some tubes at currents around 0.1 μÅ; and a poorer absolute sensitivity stability than other photomultipliers (however the relative sensitivity, i.e., color differences, is very stable). The cathode also requires an extremely high vacuum for proper operation, and any gas leakage via the metal pin-glass surfaces will result in sudden cathode destruction. Regular periodic use of the tube at anode currents in excess of 0.1 μÅ will result in slow permanent loss in photocathode sensitivity; experience has shown sensitivity losses of 2–3 over a two-year period.

The Varian tube has a unique solid photocathode with high blue sensitivity like an S20 tube, and a sensitivity beyond 1 μ which is 20 times that of a good Sl tube. It is an ideal tube to use for the Johnson (1966) *UBVRI* system, and could be used for an exact match to the Cousins or Kron *VRI* system with a red-cutoff filter at 0.88 μ. The tube should always be kept at a temperature below $-20°$ C and used at anode currents less than 1 μÅ (~ 3×10^6 Hz at a gain of 10^6), otherwise a slow, permanent loss of cathode sensitivity will result.

For most astronomical problems the more restricted wavelength responses of the GaAs or the extended S20 cathodes are adequate. The Varian tube however, will permit for the first time the measurement of the continuum color (0.75 μ-1 μ) and red-band strengths of faint galactic M dwarfs (Mould and McElroy 1978), and the extragalactic M giants, using narrow-band filters such as those of the Wing (1971) system.

TABLE V

SPECIFICATIONS OF THREE PHOTOMULTIPLIERS AT -78° C

	EMI 9658 R	RCA 31034 A-02	Varian LSE 164-A2
QE % at 0.3 μ	20	14	21
0.4 μ	23	13	18
0.6 μ	12	14	11
0.8 μ	3.5	14	5.5
1.0 μ			3
cathode size	10 mm dia	4 mm x 10 mm	5.6 mm x 6.4 mm
effective red cutoff	0.90 μ	0.87 μ	1.10 μ
dark count HZ	< 2	< 2	< 1
HV for gain 10^6	1600 V	1600 V	2600 V
special requirements		< 300 Khz	< 3 Mhz T < -20° C
selection	7% QE @ 0.7μ	dark < 12 hz	Typical tube?
approx. cost	$ 930	$1100	$6000
delivery time	6 months	6 months	6 months

NOTES:

1. The steep red cutoffs of the RCA and Varian tubes are sensitive to temperature, shifting blueward with decreasing temperature about 5 Å/°C for the Varian tube and 2 Å/°C for the RCA tube.

2. The 50 mm diameter cathode of the EMI tube was effectively reduced to reduce dark counts by attaching an annular magnet to the cathode face plate.

3. Tube selection takes time with low-volume-production tubes and the long delivery times are due to this. The Varian tube was not specially selected but has QE higher than the minimum for a typical tube. Tubes can be ordered with a specific QE at a specified red cutoff above 1.06 μ for an additional cost exceeding $1000. Varian also sell a side window version of the tube (LSE 159) for less than half the price of the 164. Its dark count is a little higher.

4. The QE calibration of the EMI and Varian tubes were provided with the tubes. The relative response of the RCA tube is from Cole and Ryer (1972) normalized with the calibrated QE at λ 0.86μ.

B. *Electronic Area Detectors*

In Table VI are given some specifications for an RCA ISIT camera tube and a Fairchild 211 CCD array. Both these devices, after careful engineering, are in regular use at KPNO and are used for quantitative work (Butcher 1978*a*,*b*). The ISIT is an essentially quantum-noise-limited detector and is very suitable for narrow-band filter work. However, the extended-red

TABLE VI

SPECIFICATIONS OF TWO AREA DETECTORS

	RCA-4849 A (ISIT)	Fairchild CCD 211
size	9.6 mm x 12.8 mm	4.4 mm x 5.7 mm
QE at 0.4 μ	13	10
0.6 μ	6.5	17
0.8 μ	2.5	22
1.0 μ	0	8.5
red cutoff	0.9 μ	1.1 μ
temperature	-20°C	-112°C
no. of pixel	256 x 256	190 x 244
pixel area	1400 μ^2	500 μ^2
scan rate	1.6 sec	integrating device
system noise for 1500 μ^2	1 count/42 reads	60 counts

Notes:

1. The violet response of the ISIT was determined by the glass fibers on the image tube face plate. A proximity-focused image tube optically contacted to the cathode of the image tube would provide UV response.
2. The CCD array has aluminum stripping covering its vertical shift registers thus optically masking half the detector area. This effectively reduces by one half the QE numbers given above.
3. The QE of the CCD was measured at KPNO. The QE of the ISIT is a typical curve from the RCA data sheets.

S20 version (like the photomultiplier) can also be used for accurate broad-band *BVRI* photometry using glass combination filters similar to those discussed above. In order to obtain photometric data, the observed field must be carefully corrected for the complicated geometrical distortion caused by the electric and magnetic fields of the image tube and TV tube, and also corrected for the sensitivity variations across the field caused primarily by the telescope illumination and the refractive properties of the input fiber optic bundles. All these effects are relatively stable under carefully engineered conditions, which include constant gain. This gain is optimized for faint objects and hence sets an upper limit to the brightness of objects that can be measured.

But although the geometric distortion and sensitivity variations can be stabilized spatially and algebraically with careful engineering, the flat-field corrections are large, vary with wavelength, and must be measured to high precision in order to realize accurate photometry of objects throughout the field (e.g., Young 1974). These corrections are the major limitations on the accuracy of ISIT camera photometry, but when done properly, photometry accurate to a few percent should be possible (Butcher 1978*a*). When exposures with different filters are taken sequentially, the geometric distortions should be identical and therefore have no effect on the precision of the magnitude differences or "colors".

The CCD array is one of a promising range of devices under continuing commercial development which utilize the very high quantum efficiency (QE) of silicon photoreceptors. The system stability is high, flat-field corrections remaining constant over several days. The main limitations of the CCD system at present are a system noise (read out noise) of 20 electrons per pixel, low quantum efficiency in the violet, reduced overall efficiency due to the presence of shielded readout registers interleaved with the light sensing sites, and the confusion of cosmic ray detections, approximately one per minute with amplitudes of several thousand electrons (Butcher 1978*b*).

For broad-band work in the near IR (0.7 μ–1.1 μ), the system noise will be dominated by the sky (for normal exposure times) and at these wavelengths also, the QE of the CCD greatly exceeds that of any alternative detector. It is therefore the best device to use at those wavelengths. The cosmic ray events will probably have to be subtracted by statistical analysis techniques, i.e., breaking up the exposure into several parts and comparing the different frames. Further development should reduce the other limitations mentioned above and the CCD arrays will probably be the main electronic area detectors within a few years.

Electron bombarded CCD arrays, i.e., intensifier tubes using CCD arrays in place of the traditional phosphors, are also being investigated by several manufacturers, Science Applications, Inc., ITT, and Varian. Varian is testing such tubes with semitransparent photocathodes having 20% QE between 0.60 μ and 0.86 μ, and is developing a similar cathode to work between 0.8 μ and 1 μ. The advantage of these tubes is that they are quantum-noise limited at lower flux levels. Varian claims that their tubes show no deleterious effects due to electron bombardment of the silicon substrate.

C. *Photographic Plates*

A great advantage of photographic plates is their large size compared to the other area detectors discussed. Even if we consider a pixel of a III a-J plate as being an area of 1500 μ^2 (a resolution element is $\sim$ 50 μ^2), a 16-cm square plate becomes a 4096 $\times$ 4096 pixel array. Such a pixel, when exposed to a density of between 1 and 2.5, has a signal-to-noise ratio of 50 on hypersensitized III a-J or III a-F plates and approximately half that on $AgNO_3$ sensitized IV-N plates. Unlike the ISIT camera tube or CCD array the photographic plates are not linear detectors but they can be accurately calibrated photographically with some care (e.g., Hoag 1978). Photographic plates show large-scale nonuniformities, or sensitivity variations due to nonuniform development or emulsion variations, which limit the absolute photometric accuracy. These nonuniformities can be effectively eliminated by making a "flat-field" exposure using a novel grid technique (Latham 1978), which is suitable for very precise area photometry. Stellar photometry could possibly also be improved in uncrowded fields by using the variations in sky background to derive the large-scale sensitivity fluctuations. But ignoring such effects, and using straight-forward two-concentric-aperture photometry of the digitized III a-J plate measured with a PDS microphotometer, Illingworth (1978) has measured magnitudes with an accuracy of 0.03 magnitude for stars between 19 and 20.5 magnitudes from a single blue III a-J plate at the $f/2.8$ prime focus of the 4-m telescope (53 μ arc sec^{-1}). Lower precision is obtained between 17–19 magnitudes and 20.5–22.5 magnitudes. Perhaps fitting profiles to the stellar images and attempting to correct for the large-scale nonuniformities of the plate one could more closely approach the $0^m.01$ level the stellar image area (1 arc sec^2) would imply; but with careful calibration and processing, only a moderate amount of computer time, and over a very limited dynamic range $0^m.03$ at present appears to be the limiting accuracy of stellar photographic photometry from a single plate.

With the recent hypersensitizing techniques, sky limited exposures can be obtained in reasonable times for plates of all the different spectral sensitizations. This

TABLE VII

PLATE AND FILTER COMBINATIONS AND NIGHTSKY BRIGHTNESS

Mag	Plates	Filters	Range μ	Δ λ Å	Av. Sky R	Total Sky R	Relative Brightness mag arcsec^{-2}	Standard Magnitudes mag arcsec^{-2}	Sky Limited Exposure f/2.8
U	III aJ +	3UG 5	~0.34-0.39	450	0.6	270	23.5	22.2	120^m
B	III aJ +	2GG 385	0.39-0.53	1400	0.5	700	22.5	22.5	45^m
V	III aF +	1GG 495 1BG 18	0.50-0.60	1000	0.8	800	22.4	22.2	60^m
V*	III aF +	2GG 495	0.50-0.70	2000	0.9	1800	21.5	21.2	25^m
R	III aF +	2RG 610	0.62-0.70	800	1.0	800	22.4	21.9	45^m
I	IV-N +	2RG 695	0.70-0.90	2000	6.0	12000	19.5	18.8	45^m
1μ	1-Z +	2RG 860	0.86-1.10	2400	34.0	82000	17.4	16.6	90^m

Notes: 1. III aJ and III aF hypersensitized with H_2, IV-N and 1-Z hypersensitized with $AgNO_3$ solution (Schoening, 1978).

2. Sensitized III aJ and III aF plates have maximum S/N of 60 for 1500 μ^2 of emulsion (Furenlid, 1978), $AgNO_3$ sensitized IV-N plates have a maximum S/N of 30 (Schoening, 1978).

TABLE VIII

FILTERS FOR UBVR I PHOTOGRAPHIC MATCH

Color	Plate-filter combination
U	III aJ + 3 mm UG 5
B	III aJ + 1 mm BG 28 + 2 mm GG 385
V	III aF + 1 mm BG 18 + 2 mm GG 495
R	III aF + 3 mm OG 590
I	IV-N + 3 mm RG N9

(Table VII) is not a reflection of the similar quantum efficiency of the different plates, but rather of the rapidly increasing sky brightness beyond 7000 Å (Fig. 11). In fact, if we accept that the III a-J plate has a peak QE of 1.5%, the IV-N plate would appear to be about 0.1% and the 1-Z plate less than 0.015%.

By using glass combination filters it is possible to duplicate closely the response of the *UBV* R_cI_c system with the III a-J, III a-F, and IV-N plates (see Table VIII); Figure 11 shows how closely the red cutoff of the IV-N plate and the GaAs photocathode are matched. However, for the faintest observations, the greater response of the *B* and *V** combination given in Table VII is preferred, although it involves nonlinear transformations onto the standard photometric system. The abrupt large increase in sky brightness past 0.8 μ due to OH molecules makes most longer-wavelength observations unprofitable, especially as the photographic *I* magnitude permits the ready detection of faint M stars or highly reddened objects by comparison with *B* or *V* magnitudes without having to go to longer wavelengths. As noted before, the $(V-I)$ index or its photographic equivalent is an excellent temperature index except when any excess sky brightness is a problem. For these faintest objects however, an alternate $(G-R)$ index ($G \equiv$ III a-J + 2 mm GG 455; $R \equiv$ III a-F + 2 mm RG 610) is suggested. This index avoids the rapid sky increase and is less line-blanketing sensitive than $(B-V)$. To measure better the metal-line (and CN band) blanketing, a violet color similar to the C of the Washington system is recommended, as it will be more metal sensitive than *B* and more photon-sensitive than *U*. This could be measured with the combination $C \equiv$ III a-J + 2 mm BG 3.

With regard to other photometric systems, the lower precision of multi-imaging photometry (photographic or electronic) precludes the utilization of the Strömgren four-color or the DDO intermediate-band system. Both these systems require 1% photometry to maintain their advantages over broad-band photometry.

VIII. Synthetic Color Indices from Digital Spectra

We have successfully computed color indices in the *UBV*, DDO, or *uvby* systems for faint stars using digital sky-subtracted spectra obtained from the IPCS at the Anglo-Australian Observatory, or the image-tube-

intensified reticon pulse-counting system at Mount Stromlo Observatory. Both systems use S20 photocathodes. The observed spectra were placed on a relatively-absolute intensity scale by observing an Oke (1974) white-dwarf photometric standard. Spectra were also obtained of "standard" stars, having known broad- or intermediate-band color indices. The relatively-absolute digital spectra were convolved with the filter responses of various photometric systems and synthetic color indices produced by applying the known transformation equations.

It was generally found necessary to compare the synthetic indices with the known color indices of the "standard" stars in order to determine the transformation equations for each night's observation. This was mainly because of the difficulties in placing the spectra on a precise relatively-absolute intensity scale.

To obtain accurate color indices it is advisable to obtain slitless spectra, so when a slit-limited higher-dispersion spectrum is taken, a much lower signal-to-noise ratio slitless spectrum should also be obtained. These two spectra can then be smoothed over long wavelength intervals and divided, so as to eliminate the effects of atmospheric dispersion on the slit spectrum.

The obtaining of digital spectra can be a versatile and efficient data-gathering procedure as one can derive radial velocities and standard color indices as well as line or band strengths.

However, to capitalize fully on these advantages it will probably be necessary to design more efficient spectrographs which maximize throughput, rather than the number of different dispersions available.

IX. Concluding Remarks

The Cousins *VRI* system defined in terms of V, $(R-I)$, and $(V-I)$ is a very precisely defined system. The primary Southern Hemisphere E-region standards are known to be accurate to a few thousandths of a magnitude, and the color indices of a set of bright equatorial stars, which are suitable for transferring the system to the Northern Hemisphere, are defined to better than 0.01 magnitude. Any future work to extend the list of secondary standards to fainter stars should maintain the precision of the system, and this would be aided by publishing color indices to the nearest thousandth of a magnitude.

Although the response of the RCA GaAs photocathode is natural to the Cousins system, good transformations are possible using the extended-red S20 or ERMA photocathodes. This is an important consideration because many observations require the advantages (i.e., large size and uniform sensitivity, semi-transparent nature or high cathode current) of these materials.

Obtaining color indices and magnitudes for faint stars will be greatly facilitated by the use of multi-imaging area detectors such as photographic plates, TV tubes, or CCD arrays. The TV tubes and solid-state arrays are linear detectors, but will still require color calibration using photoelectric standard stars. Because of the limited dynamic range and the small size of these detectors, the standard stars will need to be faint, and restricted to very small regions (< 2 arc sec) in different areas around the sky. Several globular-cluster fields have been chosen and it is hoped that stars between 14th and 17th magnitude, covering a range in color, will be measured photoelectrically in V, $(B-V)$, $(R-I)_c$, and $(V-I)_c$. Neutral density filters would then enable these fields to be used for calibration even with the largest aperture telescope.

I wish to thank Dr. A. W. Cousins for generously providing a list of equatorial stars for use as northern standards. The advice of Wieslaw Wisniewski, Ingemar Furenlid, William Schoening, Garth Illingworth, David Crawford, and especially Harvey Butcher is greatly appreciated. Valuable technical information was provided by the photomultiplier divisions of Varian LSE, RCA, and E.M.I. Gencom, Inc. Finally, I wish to thank Dr. G. R. Burbidge, the director of Kitt Peak National Observatory, for the hospitality of the Observatory where this paper was prepared. Kitt Peak National Observatory is operated by the Association of Universities for Research in Astronomy, Inc., under contract with the National Science Foundation.

REFERENCES

Auman, J. R. 1969, *Ap. J.* 157, 799.
Argue, A. N. 1967, *M.N.R.A.S.* 135, 23.
Bessell, M. S. 1976, *Pub. A.S.P.* 88, 557.
Bessell, M. S., and Wickramasinghe, D. T. 1979, *Ap. J.* 227, 232.
Bessell, M. S., and Williams, S. L. 1976, *Proc. Astr. Soc. Australia* 2, 40.
Breger, M. 1976, *Ap. J. Suppl.* 32, 7.
Broadfoot, A. L., and Kendall, K. R. 1968, *J. Geophys. Res.* 73, 426.
Butcher, H. R. 1978*a*, *Kitt Peak Quarterly Reports.*
——— 1978*b* (private communication).
Canterna, R. 1976, *A.J.* 81, 228.
Code, A. D., Davis, J., Bless, R. C., and Hanbury Brown, R. 1976, *Ap. J.* 203, 417.
Cole, M., and Ryer, D. 1972, *Electro-Optical Systems Design*, June 1972, p. 16.
Cousins, A. W. J. 1971, *Royal Obs. Annals* No. 7.
——— 1974, *Mon. Notes Astron. Soc. South Africa* 33, 149.
——— 1976*a*, *Mem. R.A.S.* 81, 25.
——— 1976*b*, *Mon. Notes Astron. Soc. South. Africa* 35, 70.
——— 1978*a*, *ibid.* 37, 8.
——— 1978*b*, *The Observatory* 98, 54.
——— 1978*c*, *Mon. Notes Astron. Soc. South. Africa* 37, 62.
——— 1979, *South African Astron. Obs. Circ.* (in press).
Cousins, A. W. J., and Jones, D. H. P. 1976, *Mem. R.A.S.* 81, 1, 23.
Crawford, D. L. 1978 (private communication).
——— 1979, Paper presented at the symposium *Important Advances in 20th Century Astronomy*, Copenhagen, 1978.

Dahn, C. C., and Guetter, H. H. 1979 (private communication).
Davis, J., and Shobbrook, R. R. 1977, *M.N.R.A.S.* 178, 651.
Dean, J. F., Warren, P. R., and Cousins, A. W. J. 1978, *M.N.R.A.S.* 183, 569.
Eggen, O. J. 1975, *Pub. A.S.P.* 87, 107.
——— 1977, *Ap. J.* 215, 812.
——— 1978, *Ap. J. Suppl.* 37, 249.
——— 1979, *ibid.* 39, 89.
Furenlid, I. 1978, in *Modern Techniques in Astronomical Photography*, R. M. West and J. L. Heudier, eds. (Geneva: European Southern Obs.), p. 153.
Gradie, J., Tedesco, E., and Zellner, B. 1978, *Bull. A.A.S.* 10, 594.
Graham, J. A. 1977 (private communication).
Hayes, D. S. 1970, *Ap. J.* 159, 165.
Hayes, D. S., and Latham, D. W. 1975, *Ap. J.* 197, 593.
Hoag, A. A. 1978, in *Modern Techniques in Astronomical Photography*, (R. M. West and J. L. Heudier, eds. (Geneva: European Southern Obs.), p. 121.
Illingworth, G. 1978 (private communication).
Jacobsen, P. U. 1970, *Astr. and Ap.* 4, 302.
Johnson, H. L. 1965, *Ap. J.* 141, 170.
——— 1966, *Ann. Rev. Astr. and Ap.* 3, 193.
——— 1978, *Rev. Mex. de Astron. y Astrof.* 4, 3.
Johnson, H. L., Mitchell, R. T., Iriarte, B., and Wisniewski, W. A. 1966, *Comm. Lunar and Planetary Lab.*, No. 63.
Kodak 1973, *Kodak Plates and Films for Scientific Photography:* Publication P 315.
Kron, G. E., and Mayall, N. U. 1960, *A.J.* 65, 581.
Kron, G. E., Gascoigne, S. C. B., and White, A. S. 1957, *A.J.* 62, 205.
Kron, G. E., Guetter, H. H., and Riepe, B. Y. 1972, *U.S. Naval Obs. Pub.* 20, part V.
Kunkel, W. E., and Rydgren, A. E. 1979, *A.J.* 84, 633.
Landolt, A. U. 1973, *A.J.* 78, 959.
——— 1978 (private communication).
Latham, D. W. 1978, in *Modern Techniques in Astronomical Photography*, R. M. West and J. L. Heudier, eds. (Geneva: European Southern Obs.), p. 141.
Lindemann, E., and Hauck, B. 1973, *Astr. and Ap. Suppl.* 11, 119.
Mould, J. R. 1976, *Astr. and Ap.* 48, 443.
Mould, J. R., and Hyland, A. R. 1976, *Ap. J.* 208, 399.
Mould, J. R., and McElroy, D. B. 1978, *Ap. J.* 220, 935.
Oke, J. B. 1974, *Ap. J. Suppl.* 27, 21.
Persson, S. E., Aaronson, M., and Frogel, J. A. 1977, *A.J.* 82, 729.
Ridgway, S. T., Joyce, R. R., White, N. M., and Wing, R. F. 1979 (preprint).
Schoening, W. E. 1978, in *Modern Techniques in Astronomical Photography* (R. M. West and J. L. Heudier, eds. (Geneva: European Southern Obs.), p. 63.
Shobbrook, R. R. 1976, *M.N.R.A.S.* 176, 673.
Thomas, J. A., Hyland, A. R., and Robinson, G. 1973, *M.N.R.A.S.* 165, 159.
Veeder, G. J. 1974, *Ap. J.* 79, 1056.
Weistrop, D. 1975, *Pub. A.S.P.* 87, 367.
Wing, R. F. 1971, in *Proceedings of the Conference on Late Type Stars* G. W. Lockwood and H. M. Dyck, eds. (Tucson: Kitt Peak National Obs.), contr. No. 554, p. 145.
Young, A. A. 1974, *Icarus* 21, 262.

APPENDIX 1

Details of *UBVRI* and 104 Photometry

A. *UBV*

Numerical simulations of natural photometric systems including *UBV* are discussed by Cousins and Jones (1976). They describe complications due to transmission of the atmosphere, the reflectivity of telescope mirrors, the transmission of color filters, and the spectral response of photomultipliers.

Cousins (1971) gives details of the tie-in of the V, $(U-B)$, and $(B-V)$ values for the equatorial stars to the Johnson system. The observed effects on $(U-B)$ of using quartz optics, glass optics, UG2 filter glass, and Corning 9863 glass are also discussed.

Part of the short-wavelength cutoff in the original Johnson U sensitivity function was due to the glass envelope of the 1P21. Table 1.I gives the transmission properties measured for a glass envelope.

Although the inclusion of a piece of glass with similar transmission properties will undoubtedly improve the match of the U response of a quartz photometer to the standard U, it is probably best to observe a set of standard stars using a range of glass thicknesses and choose the thickness which best matches standard U.

B. R_c *and* I_c

The standard R_c bandpass is primarily defined by the transmission of the two glasses comprising the filter. We followed Cousin's recipe but were unable to duplicate the R_c response, our filter transmitting too much light from red stars. By tracing our sample of KG3 glass we found that a thickness of 3 mm was necessary to match the catalog transmission of 2 mm of KG3. It may be necessary therefore to experiment with different thicknesses of the infrared-absorbing glass to produce a good match to R_c.

The standard I_c bandpass is defined by the transmission of 3 mm of RG9 and the sensitivity cutoff of an RCA 31034 tube. Cousins "standard tube" was cooled to only $-10°$ C which results in a slightly redder cutoff compared to similar tubes cooled to $-78°$ C.

TABLE 1.I

TRANSMISSION OF A 1P21 GLASS ENVELOPE

λ	T	λ	T	λ	T
0.30 μ	0.04	0.33 μ	0.77	0.36 μ	0.98
0.31 μ	0.23	0.34 μ	0.88	0.37 μ	0.99
0.32 μ	0.51	0.35 μ	0.95	0.39 μ	1.00

TABLE 1.II

FILTER TRANSMISSIONS AND NORMALIZED CATHODE RESPONSE

R		I		Cathode response*		
λ μ	T %	λ μ	T %	λ μ	−75°C %	−10°C %
0.56	9	0.70	0	0.50	55	55
0.57	46	0.71	6	0.60	72	72
0.58	71	0.72	26	0.70	92	92
0.59	77	0.73	49	0.80	99	99
0.60	77	0.74	68	0.81	100	100
0.65	65	0.75	78	0.82	99	100
0.70	45	0.77	84	0.83	97	100
0.75	25	0.79	86	0.84	94	100
0.80	11	0.81	85	0.85	78	99
0.85	4	0.85	84	0.86	47	82
0.90	1	0.90	80	0.87	10	56
		1.00	61	0.88		13
		1.10	19	0.89		4
		1.20	1	0.90		

*No tubes used were actually measured. Tabulated response is interpolated from graphical data of Cole and Ryer (1972).

TABLE 1.III

COMPARISON OF R I BANDS

Author	Band	Effective Wavelength μ	Bandpass μ	Band	Effective Wavelength μ	Bandpass μ
Cousins	R_C	0.64	0.57-0.72	I_C	0.79	0.725-0.875
Eggen	R_K	0.635	0.55-0.72	I_K	0.79	0.72 -0.865
Canterna	T_1	0.633	0.59-0.67	T_2	0.79	0.725-0.865
Kron *et al.*	R_K*	0.65	0.56-0.74	I_K	0.825	0.75 -0.90
Johnson	R_J	0.70	0.58-0.79	I_J	0.90	0.75 -0.98
Stebbins and Kron	R_6	0.72	0.65-0.78	I_6	0.98	0.90 -1.06

*The Kron, Gascoigne and White catalog was observed using this R band, but this natural color was transformed to a standard system which was defined using an R filter with a redder bandpass (0.56 μ - 0.80 μ).

This is unfortunate, but it does not appear to greatly affect the ability to reproduce the standard I_c.

The transmission of the filters which gave a reasonable match to the standard colors are given in Table 1.II.

In Table 1.III is presented a comparison of those near IR photometric systems defined by large sets of data. The bandpass limits given are the wavelengths where the transmission is 50% of the maximum within the band.

Knowledge of what absorption lines and bands fall within the bandpasses of the different systems is necessary when interpreting color indices which have been transformed from one system to another. The close relationship between the *R* and *I* bands of the Cousins and the Eggen-Kron systems should ensure that the color indices will transform faithfully (or astrophysically) even for the late-M stars. This is particularly important because of Eggen's extensive observations of the *RI* colors of M giants and dwarfs which in effect define that field.

Transformations from the other systems to Cousins should be valid for most stars except the M, R, S, and N stars, but uncertainties will always arise when dealing with objects such as weak-line stars, emission-line objects, reddened stars, and continuum objects, which are not represented in the data with which the transformations are defined. For this reason it is best to duplicate as closely as possible the natural response of the system whose data one wishes to use for comparison.

When using detectors with a redder response than the RCA 31034, the red cutoff of the R_c band can be duplicated by using a multilayer coating which reflects all light beyond 0.87 μ. Most interference filter manufacturers can produce such a filter.

C. *The 104 Band*

The restriction of the *I* band to wavelengths blueward of 0.90 μ opens up a gap in the wavelength coverage of the broad-band photometric system between I_c (0.81 μ) and *J* (1.25 μ). Such a gap would be very appropriately covered by the introduction of a new band 104, having an effective wavelength near 1.04 μ and a width (FWHM) of 0.10 μ to 0.12 μ.

The 104 band could be defined using the transmission of 2 mm of RG 1000 and the sensitivity cutoff of an Sl photocathode or a Varian type A2 photocathode, but it is probably best to use a broad-band four-period interference filter which can define the band within the sensitivity range of the detector. The Z filter of the proposed eight-color asteroid photometric system (Gradie, Tedesco, and Zellner 1978) is a very similar interference filter and it is already available at several observatories.

The advantages of the 104 band for stars, is that it avoids the confluence of Paschen lines in early-type stars and by also avoiding the strongest TiO bands is a continuum point in all but the extreme M stars. It also has an effective wavelength close to that of the photographic 1-Z band.

D. *Transformation Equations*

Cousins $(V-I)$ and $(R-I)$ standard color indices are defined by

$$(R-I)_c = 1.00\,(r-i) + \text{const}$$

and

$$(V-I)_c = 0.973\,(V-i) + \text{const}\quad,$$

where *r*, *i* are the instrumental magnitudes using his glass filters and RCA 31034 A tube cooled to −10° C. At KPNO using the filters recommended earlier, the transformations derived with one RCA 31034 A tube (at −78° C) were

Non-M stars	M stars
$B-V = 1.00\ (b-v) - 0.17$	$B-V = 1.10\ (b-v) - 0.34$
$R-I = 1.063\,(r-i) + 0.82$	$R-I = 1.036\,(r-i) + 0.815$
$V-I = 1.067\,(v-i) + 0.94$	$V-I = 1.00\ (v-i) + 0.97$

$$V = v + 0.03\,(B-V)$$

APPENDIX 2
Absolute Calibration of $UBVR_cI_c$ and 104

Cousins has measured color indices for 22 stars listed in the Breger (1976) spectrophotometric catalog including eight of the Hayes (1970) secondary standards. Synthetic color indices were computed from the absolute fluxes using normalized sensitivity functions taken from Table 1.II, and these were compared with the observed indices to yield absolute color differences for a fictitious star with $(V-R)$ and $(R-I)$ indices of zero. The U and B differences were not calculated this way because the flux distributions which were used avoided the hydrogen lines and the Balmer discontinuity. For these bands it was decided to use the color indices and energy distribution of the B supergiant ϵ Orionis which has little evidence of a Balmer discontinuity or strong absorption lines. For ϵ Ori, Cousins gives $(U-V) = 1^m.23$ and $(B-V) = -0^m.19$; the scans give $(M_{0.355} - m_{0.547}) = -0.47$ and $(m_{0.433} - m_{0.547}) = -0.36$. From all these comparisons one can derive the absolute magnitude differences given in Table 2.IV.

The measurements for α Lyrae itself were used to derive the V magnitude calibration, and the V-104 (probable) calibration was derived from θ Virginis.

For α Lyr $V = 0^m.03$ (Johnson et al. 1966) and at $\lambda 5556$ $F_\nu = 3.50 \times 10^{-23}$ W m^{-2} Hz^{-1} (Hayes and Latham, 1975). The scans show that

$$m_{0.548} - m_{0.556} = -0.012 \quad ,$$

therefore at the effective wavelength of V, a $V = 0$ star has a flux of

$$F_\nu = 3.64 \times 10^{-23} \text{ W m}^{-2} \text{ Hz}^{-1} \quad .$$

Cousins' color indices show that θ Vir has indices close to the fictitious zero magnitude index star, therefore we adopt $V-104 = 0.00$ also. For θ Vir

$$m_{0.55} - m_{1.04} = -0.584 \quad .$$

From the strength of the hydrogen lines and the continuum slope given by Johnson (1978) for α Lyr it can be anticipated that the 104 band will measure an intensity about 7% lower than the 1.04 μ continuum point. The absolute magnitude difference for $V - 104$ is therefore -0.654 magnitude.

The $(V-K)$ calibration was adopted from Thomas, Hyland, and Robinson (1973).

TABLE 2.IV

ABSOLUTE MAGNITUDE DIFFERENCES

	U-V	B-V	V-R	V-I
Absolute color index	0.76	-0.17	-0.18	-0.39
Standard color index	0.00	0.00	0.00	0.00

APPENDIX 3
The Effective Wavelengths of V_J, R_c, and I_c

The effective wavelengths of V_J, R_c, and I_c for stars of different colors, which were also calculated from the absolute fluxes, are given in Table 3.V. They show that λ_{eff} for V and I_c changes by less than 100 Å between A0 and M0 spectral type, while R_c changes by more than 800 Å. This large change in R_{eff} must be considered when deriving reddening curves for $(V-R)$ and $(R-I)$, and when using R for absolute flux measurements. The effective wavelength change will be slightly larger for Eggen's R_K band which is slightly wider than R_c.

TABLE 3.V

Effective Wavelengths of V, R_C, and I_C

MK	V	R_C	I_C
A0	0.542	0.638	0.787
G0	0.547	0.653	0.789
K5	0.549	0.676	0.791
M0	0.551	0.722	0.795